Heliyon 6 (2020) e05776

Contents lists available at ScienceDirect

Heliyon

journal homepage: www.cell.com/heliyon

Research article

A molecular scale analysis of TEMPO-oxidation of native cellulose molecules

Milad Asgarpour Khansary [a,b,*], Peyman Pouresmaeel-Selakjani [c], Mohammad Ali Aroon [d], Ahmad Hallajisani [e], Jennifer Cookman [f], Saeed Shirazian [b]

[a] Confirm Smart Manufacturing Center, Bernal Institute, University of Limerick, Limerick, Ireland
[b] Department of Chemical Sciences, Bernal Institute, University of Limerick, Limerick, Ireland
[c] Young Researcher and Elite Club, Rasht Branch, Islamic Azad University, Rasht, Iran
[d] Membrane Research Laboratory, Caspian Faculty of Engineering, College of Engineering, University of Tehran, Tehran , Iran
[e] Biofuel Research Laboratory, Caspian Faculty of Engineering, College of Engineering, University of Tehran, Tehran , Iran
[f] Bernal Institute, University of Limerick, Limerick, Ireland

ARTICLE INFO

Keywords:
Cellulose
TEMPO oxidation
Density functional theory
Molecular dynamics
Surface modification

ABSTRACT

The native cellulose, through TEMPO (2,2,6,6-tetramethylpiperidine-1-oxyl radical)-mediated oxidation, can be converted into individual fibers. It has been observed that oxidized fibers disperse completely and individually in water. It is believed that electrostatic repulsive forces might be responsible for such observations. In order to study the TEMPO-oxidation of cellulose molecules, we used Density Functional Theory (DFT) calculations and Flory-Huggins theory combined with molecular dynamics (MD). The surface electrostatic potential in native cellulose and TEMPO-oxidized cellulose were calculated using DFT calculations. We found that TEMPO-oxidized cellulose accommodates a threefold screw conformation where the negatively charged (–COO–) functional groups are pointed away from the surface in all spatial directions. This spatial orientation causes that TEMPO-oxidized cellulose molecules repulse each other due to strong negatively charged surface. At the same time, the spatial orientation increases the hydrophilicity in TEMPO-oxidized cellulose molecules. These observations explain the improved dispersion in water and separability of TEMPO-oxidized cellulose molecules. We obtained large and positive Flory–Huggins interaction parameters for TEMPO-oxidized cellulose molecules indicating their higher dispersion once in water.

1. Introduction

One of the most abundant biomolecules on the earth is cellulose [1]. Cellulose has found applications in a wide range of industries such as pharmaceuticals, biofuel, fibers [2]. Cellulose fibrils are generally lightweight and have shown interesting properties, specifically high tensile strengths (around 200–300 MPa), and elastic moduli (around 6–7 GPa) [3, 4]. Cellulose fibrils can be produced from native cellulose through TEMPO (2,2,6,6-tetramethylpiperidine-1-oxyl radical)-mediated oxidation systems in water [5, 6, 7]. Two commonly used TEMPO-mediated oxidation processes are (i) aqueous solution of 2,2,6,6-tetramethylpiperidine-1-oxyl combined with NaBr, NaClO at pH 10–11 (see Figure S1 in SI.1) or (ii) NaClO, $NaClO_2$ at pH 4.8–6.8 (see Figure S2 in SI.1) [8]. Through TEMPO-mediated oxidation processes, primary C6–OH groups on native cellulose ($-CH_2OH$) are oxidized to sodium carboxylate groups ($-COONa$) [9, 10, 11, 12]. Isogai et al. [7] reported that a complete oxidation of C6–OH groups ($-CH_2OH$) to sodium carboxylate groups takes place. Later on, the sodium atoms dissociate from sodium carboxylate groups ($-COONa$). As a result of sodium dissociation, negatively charged carboxylate functional groups (–COO–) are left on TEMPO-oxidized cellulose.

It has been previously observed that these fibrils are not agglomerated with each other. They disperse completely as individual fibrils in water [5, 6, 7]. It is believed that electrostatic repulsive forces might be responsible for these observations. Getting experimental evidences for such forces is extremely difficult. Therefore, in order to confirm that, it is of great interest to study, on the molecular scale, how TEMPO-oxidization alters molecular structure and their interactions [13, 14]. It is worthwhile to investigate the effect of degree of oxidation of ($-CH_2OH$) group by ($-COO-$) group. Here, we used computational techniques including Density Functional Theory (DFT) calculations and molecular dynamics (MD). We employed DFT calculations to relax molecular models of native and TEMPO-oxidized molecules to get their stable structures. We determined the surface electrostatic potential in

* Corresponding author.
E-mail address: Milad.Asgarpour@ul.ie (M. Asgarpour Khansary).

https://doi.org/10.1016/j.heliyon.2020.e05776
Received 21 August 2020; Received in revised form 27 September 2020; Accepted 15 December 2020

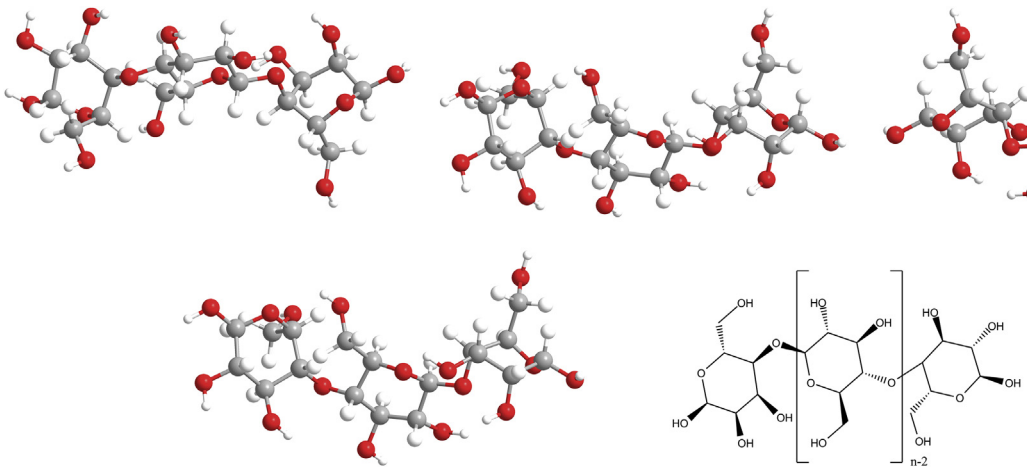

Figure 1. Repeating unit reported by Nishiyama et al. [18] used to create cellulose molecule models.

native cellulose and TEMPO-oxidized cellulose models to evaluate the structural changes and orientation of the functional groups. Additionally, we employed a Flory–Huggins theory combined with molecular dynamics to calculate molecular Flory–Huggins interaction parameters as it can be used for compatibility analysis [15, 16, 17].

2. Computational methods

2.1. Molecular model structure of native cellulose

Nishiyama et al. [18] provided the glucose residue structure (Figure 1) which is used to build our model cellulose molecules. We observed in our previous works [19, 20] that the selected unit structure provides a good representation of cellulose properties. In present work, both molecular dynamics and DFT calculations are performed. Therefore, it is necessary to avoid a large molecule due to computational costs of DFT calculations [21]. In contrast, to get reliable molecular Flory–Huggins interaction parameters from molecular dynamics, a reasonably large molecule is needed [22, 23]. Herein, the cellulose model consists of 16 glucose residues.

2.2. Molecular model structure of TEMPO-oxidized cellulose

To track the surface changes that the cellulose molecule experiences due to oxidation of different functional group contents through TEMPO-oxidation process, we created a series of cellulose variants/conformation. These variants include (1) cellulose molecules with (–CHO) functional groups, (2) cellulose molecules with (–COOH) functional groups, (3) cellulose molecules with (–COONa) functional groups and (4) cellulose molecules with ($–COO^-$). These variants are considered based on the currently accepted mechanisms as shown in Figure S1 and Figure S2 [8]. To create these model molecules, we remove the ($–CH_2OH$) groups in native cellulose and replace with the respective functional groups in each variant 1–4. Also, as sixteen $–CH_2OH$ groups are present on model native cellulose molecule, replacement of the functional groups is considered from 1 to 16. This can represent the partial oxidation toward full oxidation.

2.3. Density functional theory calculations

For all four cellulose variants detailed in the previous section, we performed structural relaxation to ensure the model molecules are stable

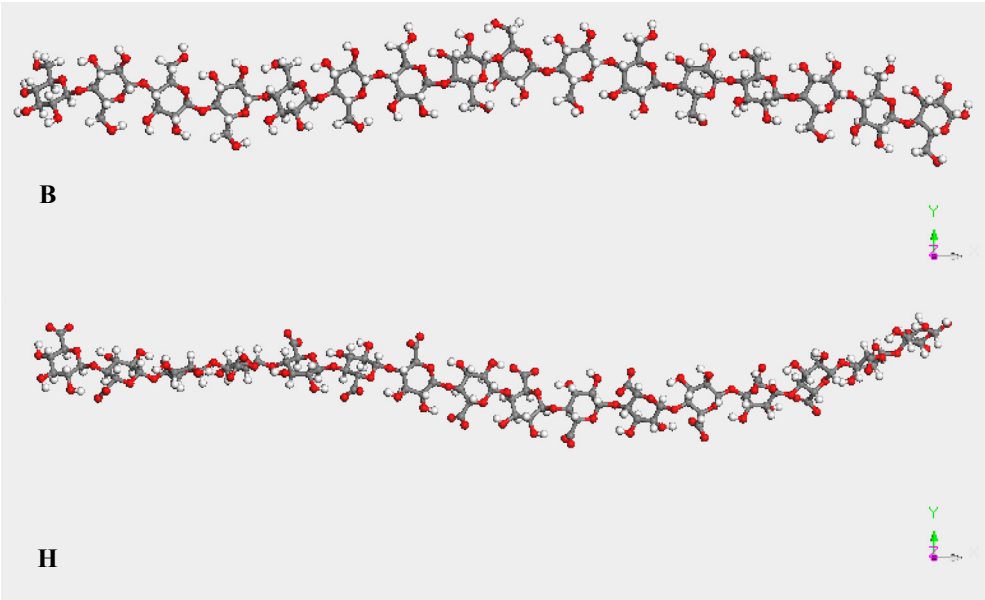

Figure 2. Relaxed structures obtained using density functional theory calculations showing conformational changes of cellulose variants: *B:* native cellulose and *H:* TEMPO-oxidized cellulose (fully oxidized).

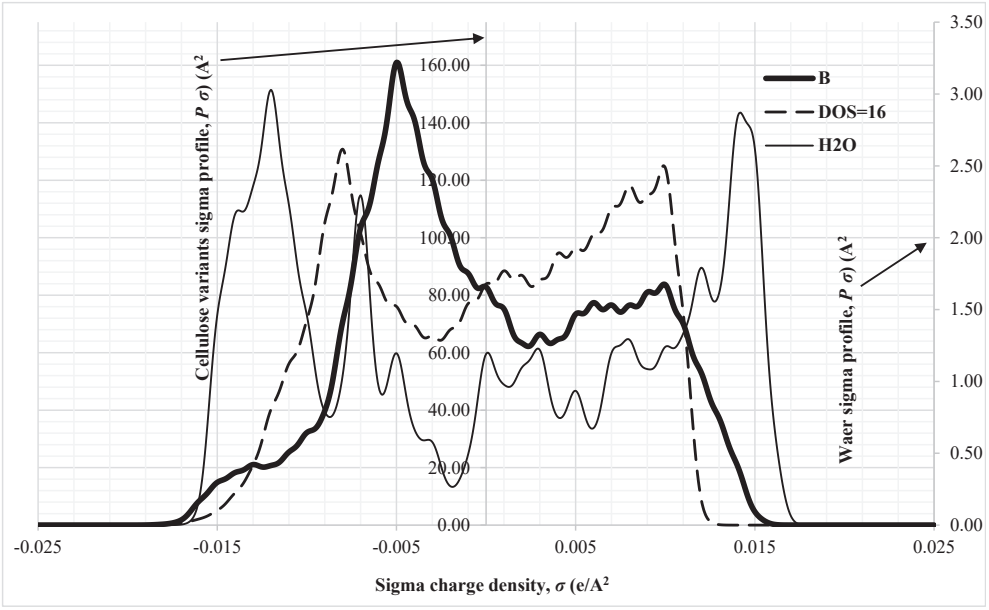

Figure 3. The COSMO surface charge density profiles of water, native cellulose (B) and fully oxidized cellulose (DOS = 16).

and at their minimum energy. For all DFT calculations performed in this work, we used the DMol^3 package. The generalized gradient approximations with Perdew-Becke-Ernzerhof (PBE) function was used as recommended [24]. Since the molecules would generally be in solution in TEMPO-oxidation process, the solvation effects must be considered via relaxation calculations. Therefore solvation effects are accounted for by implementing the COnductor-like Screening Model (COSMO) via the DMol^3 package as described by Klamt et al. [25]. To control the convergence behavior for enhanced self-consistent field calculations [26], thermal smearing [27] is applied including double numerical basis and d-polarization function level of theory. The COSMO surface charge densities are extracted from DMol^3 output files.

2.4. Flory-Huggins theory combined with molecular dynamics

The Flory–Huggins interaction parameter χ_{ij} [28] between molecule i and j is related to coordination number (Z_{ij}) and average binding energy (E_{ij_T}) as $\chi_{ij} = 0.5[Z_{ij}E_{ij_T} + Z_{ji}E_{ji_T} - Z_{ii}E_{ii_T} - Z_{jj}E_{jj_T}]/RT$ [29, 30, 31]. Here R is the universal gas constant and T is temperature. The Blend package is used to calculate the Flory-Huggins parameter [28, 30]. In order to avoid risk of improper relaxation and charge assignments using force fields, we use the relaxed structures obtained from DFT calculations as input here. The INTERFACE force field model v.1.5 is used as described by Heinz et al. [32, 33]. The Flory–Huggins interaction parameter values are extracted from Blend output files.

3. Results and discussion

3.1. Density functional theory calculations

As previously mentioned, Isogai et al. [7] suggest that a complete TEMPO-mediated oxidation process takes place i.e. full oxidation of the ($-CH_2OH$) groups by the carboxylate ($-COO^-$) groups. The corresponding results are presented herein, and the remaining data can be found in the accompanying supplementary files (see SI.2 for visualized relaxed structured, SI.3 for sigma charge density profiles and SI.5 for coordinate of atoms in each structure).

In Figure 2, the relaxed structure of native cellulose and complete TEMPO-oxidized cellulose (containing ($-COO^-$) groups) molecules are presented where conformational changes upon surface modification of cellulose can be observed. As seen in Figure 2, the complete TEMPO-oxidized cellulose accommodates a threefold screw conformation. Because of this conformation, all (–COO–) groups are pointed away from the surface of cellulose in all directions. This spatial orientation causes that TEMPO-oxidized cellulose molecules repulse each other due to strong negatively charged surface. At the same time, the spatial orientation increases the hydrophilicity in TEMPO-oxidized cellulose molecules. These observations explain the improved dispersion and separability of TEMPO-oxidized cellulose molecules. This conclusion is consistent with observations reported by Isogai et al. [7].

Table 1. The calculated values of Flory–Huggins interaction parameter, χ_{ij}, at standard temperature and pressure condition.

	H_2O	$C_5H_7O_4$	($-CH_2OH$)	(–CHO)	(–COOH)	(–COONa)	($-COO^-$)
H_2O	0						
$C_5H_7O_4$	-9.79980432	0					
($-CH_2OH$)	-1.25775834	-1.58867227	0				
(–CHO)	6.11254968	7.27009437	5.01320897	0			
(–COOH)	-14.43749519	1.73641587	-8.47843226	1.97779403	0		
(–COONa)	11.12301353	2.56198663	7.93710466	3.08680920	4.90900649	0	
($-COO^-$)	9.77825227	5.67684352	6.79519086	0.77570342	3.94728670	1.04452272	0

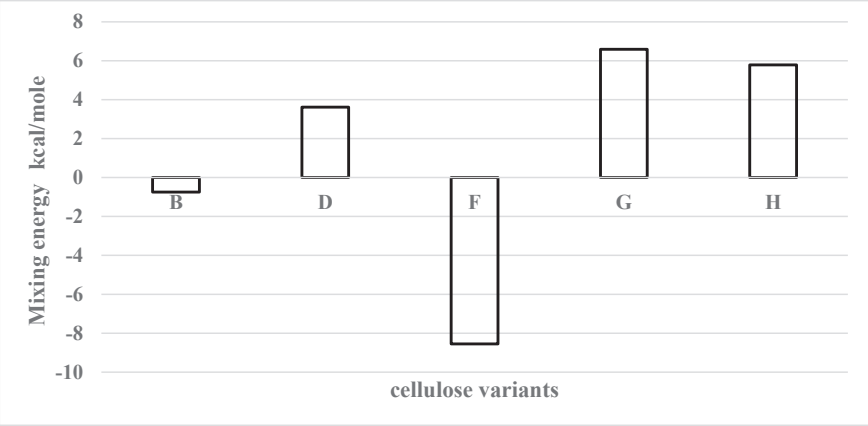

Figure 4. Mixing energies of water and cellulose variants. *B:* native cellulose, *D:* (–CHO) group containing variant, *F:* (–COOH) group containing variant, *G:* (–COONa) group containing variant and *H:* –(COO^-) group containing variant.

Finally, the obtained surface charge densities, σ, and their respective probability, $P(\sigma)$, are shown in Figure 3 for water, native cellulose, and TEMPO-oxidized cellulose (fully oxidized). For the analysis of surface charge densities, the peak from the negative lone-pairs is located on the right side and vice versa [1, 25].

A wide and symmetric profile is obtained for water which is consistent with previous studies [1, 34]. The lone-pair electrons on oxygen are responsible for the peak around $\sigma = 0.014\ e/Å^2$ in water sigma profile. The peak at $\sigma =$ -0.014 $e/Å^2$ in water sigma profile is generated by the two polar hydrogen atoms. The flat and symmetric region spanning a charge density range of -0.0079–$0.0079\ e/Å^2$ indicates the feature of water to involve in donor-acceptor electrostatic interactions. Both native cellulose and fully oxidized cellulose showed a shoulder–like peak around 0.0023 $e/Å^2$ which can be attributed to the exposed surface of carbon atoms. All model cellulose variants have this shoulder–like peaks (around 0.0023 $e/Å^2$) in common. As this peak indicates a negative charge, then a repulsive interaction could be realized for all cellulose variants. The carbon-containing pyranosyl rings are responsible for the peak at $\sigma = 0.005$ e/Å2. In fully oxidized cellulose, the lone-pair electrons on the oxygen atom in the carboxyl groups are easily distinguished due to the observed peak around $\sigma = 0.013\ e/Å^2$. The weak peak at $\sigma =$ -0.014 $e/Å^2$ in native cellulose indicates the hydrogen atoms in pyranosyl rings (that have five C and one O) as the positive charges of these hydrogen atoms are distributed over a large area. The affinity of cellulose for acting as proton donor (through hydrogen donation in CH_2OH group) is indicated by the strong peak at around $\sigma =$ -0.006 $e/Å^2$. As the hydrogen bonding is weak up to -0.002 $e/Å^2$, hydrogen donation in CH_2OH group is expected.

3.2. Flory-Huggins theory combined with molecular dynamics

The calculated values of Flory–Huggins interaction parameter, χ_{ij}, at standard temperature and pressure for each of the two molecular pairs are listed in Table 1 (also see SI.4 for further details). The Flory–Huggins interaction parameter can provide insight into the compatibility and possibility of interactions between two molecules [35]. Generally, when a small or negative value of χ is obtained, it can be concluded that two particles may have desirable attraction, and this can result in a new phase formation. Aggregation of similar particles by themselves is expected if the determined χ is large and positive. A high value of χ value shows that the mixture of two components will separate into two phases [36].

A small and negative Flory–Huggins interaction parameter is obtained for water and native cellulose pairs signifying that the native cellulose is stable in water. For the cellulose variant containing –COO^- functional group and water pairs, a large and positive χ_{ij} is obtained, meaning that the cellulose variant containing TEMPO-oxidized cellulose tends to be dispersed and won't agglomerate with each other in water. This is in agreement with the experimental observations of enhanced dispersion and easier separation of the TEMPO-oxidized cellulose [8].

In Figure 4, the averaged mixing energies of water and cellulose variants (see section 2) are displayed. Generally, the energy of mixing should always be negative where mixing is possible and spontaneous [37]. From Figure 4, it can be concluded that each cellulose variant shows different tendencies for aggregation and agglomeration. The mixing energy of the cellulose variant containing (–COO^-) functional group (fully TEMPO-oxidized cellulose) group in water suggests that this variant in water tends to disperse and stay separated which is consistent with literature [13, 14].

4. Conclusion

Computational experiments involving DFT and Flory-Huggins parameter calculations are performed to study the surface changes that occur on cellulose molecules and their effect on the properties and interaction of the molecules in solution. It is found that a threefold screw conformation results for fully oxidized cellulose, which creates a negatively charge surface. This in turn results in a completely strong electrostatic repulsion characteristics on fully oxidized cellulose. Thus, this enhances the solubility in water while makes the separation of modified cellulose much easier.

Declarations

Author contribution statement

Milad Asgarpour Khansary, Peyman Pouresmaeel-selakjani: Conceived and designed the experiments; Analyzed and interpreted the data; Wrote the paper.

Mohammad Ali Aroon, Ahmad Hallajisani, Jennifer Cookman, Saeed Shirazian: Analyzed and interpreted the data; Wrote the paper.

Funding statement

This research did not receive any specific grant from funding agencies in the public, commercial, or not-for-profit sectors.

Data availability statement

Data associated with this study has been deposited using tag ID = CNFs at https://sites.google.com/view/makhansary/downloads

Declaration of interests statement

The authors declare no conflict of interest.

Additional information

Supplementary content related to this article has been published online at https://doi.org/10.1016/j.heliyon.2020.e05776.

References

[1] A. Ghasemi, et al., Using quantum chemical modeling and calculations for evaluation of cellulose potential for estrogen micropollutants removal from water effluents, Chemosphere 178 (2017) 411–423.
[2] B. Jallabert, et al., The pressure–volume–temperature relationship of cellulose, Cellulose 20 (5) (2013) 2279–2289.
[3] A. Kafy, et al., Cellulose long fibers fabricated from cellulose nanofibers and its strong and tough characteristics, Sci. Rep. 7 (1) (2017) 17683.
[4] H. Fukuzumi, et al., Transparent and high gas barrier films of cellulose nanofibers prepared by TEMPO-mediated oxidation, Biomacromolecules 10 (1) (2009) 162–165.
[5] T. Saito, A. Isogai, TEMPO-mediated oxidation of native cellulose. The effect of oxidation conditions on chemical and crystal structures of the water-insoluble fractions, Biomacromolecules 5 (5) (2004) 1983–1989.
[6] T. Saito, et al., Cellulose nanofibers prepared by TEMPO-mediated oxidation of native cellulose, Biomacromolecules 8 (8) (2007) 2485–2491.
[7] A. Isogai, T. Saito, H. Fukuzumi, TEMPO-oxidized cellulose nanofibers, Nanoscale 3 (1) (2011) 71–85.
[8] R.J. Moon, et al., Cellulose nanomaterials review: structure, properties and nanocomposites, Chem. Soc. Rev. 40 (7) (2011) 3941–3994.
[9] A. Isogai, Y. Kato, Preparation of polyuronic acid from cellulose by TEMPO-mediated oxidation, Cellulose 5 (3) (1998) 153–164.
[10] T. Isogai, M. Yanagisawa, A. Isogai, Degrees of polymerization (DP) and DP distribution of cellouronic acids prepared from alkali-treated celluloses and ball-milled native celluloses by TEMPO-mediated oxidation, Cellulose 16 (1) (2009) 117–127.
[11] D. da Silva Perez, S. Montanari, M.R. Vignon, TEMPO-mediated oxidation of cellulose III, Biomacromolecules 4 (5) (2003) 1417–1425.
[12] T. Isogai, T. Saito, A. Isogai, TEMPO electromediated oxidation of some polysaccharides including regenerated cellulose fiber, Biomacromolecules 11 (6) (2010) 1593–1599.
[13] T. Moberg, et al., Rheological properties of nanocellulose suspensions: effects of fibril/particle dimensions and surface characteristics, Cellulose 24 (6) (2017) 2499–2510.
[14] L. Geng, et al., Rheological properties of jute-based cellulose nanofibers under different ionic conditions, in: Nanocelluloses: Their Preparation, Properties, and Applications, American Chemical Society, 2017, pp. 113–132.
[15] M. Asgarpour Khansary, M.A. Aroon, On the consistency and correctness of thermodynamics phase equilibria modeling and correlation reports published in Fuel journal, Fuel 140 (2015) 810–811.
[16] M.A. Khansary, M.A. Aroon, Reply to the comments "On the consistency and correctness of thermodynamics phase equilibria modeling and correlation reports published in Fuel journal", Fuel 142 (2015) 306–307.
[17] A. Farajnezhad, et al., Correlation of interaction parameters in Wilson, NRTL and UNIQUAC models using theoretical methods, Fluid Phase Equil. 417 (2016) 181–186.
[18] Y. Nishiyama, P. Langan, H. Chanzy, Crystal structure and hydrogen-bonding system in cellulose iβ from synchrotron X-ray and neutron fiber diffraction, J. Am. Chem. Soc. 124 (31) (2002) 9074–9082.
[19] M. Asgarpour Khansary, S. Shirazian, Theoretical modeling for thermophysical properties of cellulose: pressure/volume/temperature data, Cellulose 23 (2) (2016) 1101–1105.
[20] M. Asgarpour Khansary, M.A. Aroon, S. Shirazian, Physical adsorption of CO2 in biomass at atmospheric pressure and ambient temperature, Environ. Chem. Lett. 18 (4) (2020) 1423–1431.
[21] E. Karezani, A. Hallajisani, M. Asgarpour Khansary, A quantum mechanics/molecular mechanics (QM/MM) investigation on the mechanism of adsorptive removal of heavy metal ions by lignin: single and competitive ion adsorption, Cellulose 24 (8) (2017) 3131–3143.
[22] M.A. Khansary, A. Marjani, S. Shirazian, On the search of rigorous thermo-kinetic model for wet phase inversion technique, J. Membr. Sci. 538 (2017) 18–33.
[23] M. Asgarpour Khansary, S. Shirazian, M. Asadollahzadeh, Polymer-water partition coefficients in polymeric passive samplers, Environ. Sci. Pollut. Control Ser. 24 (3) (2017) 2627–2631.
[24] A. Dal Corso, et al., Generalized-gradient approximations to density-functional theory: a comparative study for atoms and solids, Phys. Rev. B 53 (3) (1996) 1180–1185.
[25] A. Klamt, COSMO-RS from Quantum Chemistry to Fluid Phase Thermodynamics and Drug Design, Elsevier, 2005.
[26] A.D. Rabuck, G.E. Scuseria, Improving self-consistent field convergence by varying occupation numbers, J. Chem. Phys. 110 (2) (1999) 695–700.
[27] C.R. Leavens, Effect of thermal smearing on the electron-phonon spectral function obtained by inversion of normal metal tunneling data, Solid State Commun. 54 (7) (1985) 625–628.
[28] R.D. Groot, T.J. Madden, Dynamic simulation of diblock copolymer microphase separation, J. Chem. Phys. 108 (20) (1998) 8713–8724.
[29] K.S. Schweizer, J.G. Curro, Integral equation theory of the structure and thermodynamics of polymer blends, J. Chem. Phys. 91 (8) (1989) 5059–5081.
[30] A.I. Pesci, K.F. Freed, Lattice models of polymer fluids: monomers occupying several lattice sites. II. Interaction energies, J. Chem. Phys. 90 (3) (1989) 2003–2016.
[31] A.M. Nemirovsky, M.G. Bawendi, K.F. Freed, Lattice models of polymer solutions: monomers occupying several lattice sites, J. Chem. Phys. 87 (12) (1987) 7272–7284.
[32] H. Heinz, et al., Thermodynamically consistent force fields for the assembly of inorganic, organic, and biological nanostructures: the INTERFACE force field, Langmuir 29 (6) (2013) 1754–1765.
[33] C.C. Dharmawardhana, et al., Reliable computational design of biological-inorganic materials to the large nanometer scale using Interface-FF, Mol. Simulat. 43 (13-16) (2017) 1394–1405.
[34] M.R. Islam, C.-C. Chen, COSMO-SAC sigma profile generation with conceptual segment concept, Ind. Eng. Chem. Res. (2014), 141209090605008.
[35] M.A. Khansary, Vapor pressure and Flory-Huggins interaction parameters in binary polymeric solutions, Kor. J. Chem. Eng. 33 (4) (2016) 1402–1407.
[36] L. Keshavarz, M.A. Khansary, S. Shirazian, Phase diagram of ternary polymeric solutions containing nonsolvent/solvent/polymer: theoretical calculation and experimental validation, Polymer 73 (2015) 1–8.
[37] A. Ejraei, et al., Lower and upper critical solution temperatures of binary polymeric solutions, Fluid Phase Equil. 425 (2016) 465–484.